CHARACTERIZATION OF A $\{(Fe_{60}Co_{40})_{75}B_{20}Si_5\}_{96}Nb_4$ IMPULSE ATOMIZED GLASSY POWDER BY NEUTRON DIFFRACTION AND DIFFERENTIAL SCANNING CALORIMETRY

A-A. Bogno[a], U. Dahlborg[b]; M. Calvo-Dahlborg[b]; C.Riveros[a], N. Ciftci[a, c]; H. Henein[a]

[a] Chemical and Materials Engineering, University of Alberta, Edmonton, Canada
[b] Groupe de Physique des Materiaux, CNRS-UMR6634, Universite de Rouen, Campus Madrillet, France
[c] Foundation Institute of Materials Science (IWT), Department of Production Engineering, University of Bremen, Germany

Key words: Impulse Atomization, Rapid Solidification, Iron Cobalt, BMG, Calorimetry, Neutron Diffraction

Corresponding author: bogno@ualberta.ca

Abstract

This paper investigates FeCo-based alloy glass formability by high undercooling and high cooling rate solidification technique and the hardness evaluation of the generated samples. For this investigation, Impulse Atomization was used to generate $\{(Fe_{60}Co_{40})_{75}B_{20}Si_5\}_{96}Nb_4$ powders of different sizes that correspond to different cooling rates and undercoolings. The amorphous fraction and kinetic crystallization properties of the investigated powders were determined by means of Differential Scanning Calorimetry and Neutron Diffraction. The enthalpy of crystallization of a close to amorphous powder produced by gas atomization was used as a reference for the calculation of amorphous fraction by calorimetry in atomized powders. Thus, a quantitative estimation of cooling rate corresponding to each powder size and the variation of amorphous fraction with cooling rate are presented. Higher cooling rate promoted by smaller powder size and helium atomization atmosphere is found to yield higher amorphous fraction. At relatively high cooling rates Neutron Diffraction technique yields higher amorphous fractions than the Differential Scanning Calorimetry technique. The critical cooling rate for amorphous phase formation under unconstrained solidification conditions using Impulse Atomization is found to be ~15,000Ks^{-1} which corresponds to a powder size of about 100 μm atomized in nitrogen or about 200 μm atomized in helium.

1. Introduction

Improving the properties and performance of industrial products has always been one of the main focuses of research in materials science. Thus material scientists have been putting a lot of efforts in order to reach this goal by either modifying existing materials or developing new materials. Modification of existing materials includes addition of alloying elements, microstructural modification by heat treatment etc. Developed new materials include quasi-crystals, nano-crystalline materials and metallic glasses [1-7]. Due to their many intrinsic properties, including corrosion resistance, strength, soft magnetism, and high moldability in the supercooled region, metallic glasses in general have attracted a great deal of engineering interest in recent years. The production of a metallic glass requires basically three component rules: (1) A multi-component alloy consisting of more than three elements, (2) A significant atomic size mismatches of over 12% among the main three elements, and (3) negative heats of mixing among the main three elements. This paper studies the glass formability and rapid solidification of a FeCo-base alloy powders generated by Impulse Atomization (IA) [2]. This technique is very efficient in investigating the synthesis conditions of new materials. $\{(Fe_{60}Co_{40})_{75}B_{20}Si_5\}_{96}Nb_4$ alloy was proposed by Inoue et al. [3] in 2004 with the production of fully glassy rods of up to 4mm in diameter by the ejection casting method in a copper mould. The alloy presented a supercooled liquid region $\Delta T = 50K$, denoting a very high glass-forming ability with critical cooling rates in the range of 10^1–10^2 Ks^{-1} only.

The aim of this study is twofold: First aim is to give a quantitative estimation of the amorphous fraction using two characterization techniques (i) Neutron Diffraction (ND) and (ii) Differential Scanning Calorimetry (DSC). Second aim is to estimate the cooling rate as a function of powder size so that the critical cooling rate and powder size for the formation of a fully amorphous powder under unconstrained solidification conditions can be determined. The results of study will allow better control over the use of such powders for manufacturing purposes, such as Additive Manufacturing.

2. Experimental

2.1. Powder production

In this paper, the word powder refers to a liquid droplet that has completely solidified while droplet is referred to a melt in a spherical shape. For this investigation, a pre-alloy Iron-Boron (80.5 mass% of Fe and 18.3 mass% of B), pure Co (99.7 mass %), Fe (99.63 mass %), Nb (99.9 mass %), and Si (99.8 mass %) were melted in an Al_2O_3 crucible to obtain a

$\{(Fe_{60}Co_{40})_{75}B_{20}Si_5\}_{96}Nb_4$ liquid. Powders from this liquid metal were generated by Impulse Atomization under nitrogen and helium atmospheres [4] and by gas atomization (GA) [5]. The powders considered in the present investigation were atomized from a temperature of 1500K respectively into nitrogen (abbreviated as N) and helium (abbreviated as H) containing less than 20 ppm oxygen. They were washed successively with Toluene and Ethanol. A total time of 2 days was allowed for the powders to fully dry and get rid of excess alcohol. Afterwards, the powders were sieved into different size ranges varying from a minimum size of 180µm to a maximum size of 1180µm according to the *Standard Test Method for Sieve Analysis of Metal Powders, ASTM B214, 2011*. In the present study, the size of a powder is defined as the average value of each size range. The corresponding liquid cooling rate, a parameter that depends on the atomization atmosphere (H or N) [6] is estimated for droplets in each size range using a solidification model of atomization which is described in [7]. The model assumes a uniform temperature for the entire droplet. The cooling starts at the atomization temperature and continues by heat loss to the a quiescent atmosphere (H or N) during its fall with an initial velocity of $0.5ms^{-1}$. Heat loss to the gas, mainly through convection, is a result of the relative velocity between the falling droplet and the atomization gas. Fig.1 shows the variation of liquid cooling rate with average droplet size.

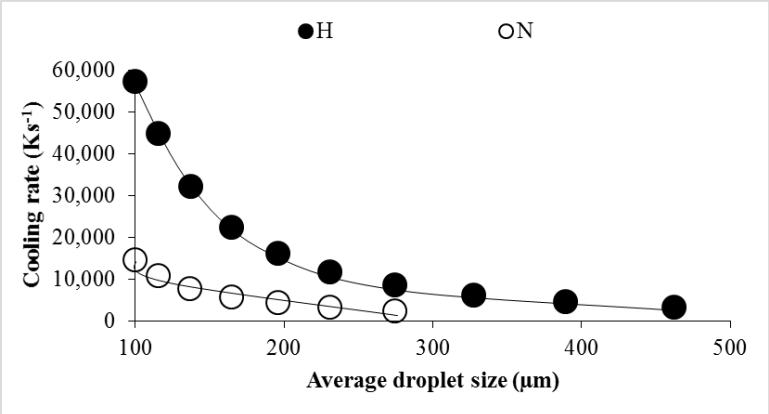

Fig.1: *Variation of the cooling rates (estimated by the Thermal model* [7] *) with average droplet size for samples atomized under helium (H) and nitrogen (N).*

As expected, cooling rate increases as droplet size decreases. Furthermore, for two droplets of the same size, the one atomized in helium yields a higher cooling rate as compared to the one atomized in nitrogen, due to a relatively higher thermal conductivity of helium. Table I shows a summary of the samples characterized by both ND and DSC with their corresponding liquid cooling rates.

Table 1: Nomenclature and characteristics of the investigated samples

	Nitrogen			Helium			
Legend	3N	8N	12N	3H	6H	9H	12H
Average droplet size (μm)	125	300	600	125	212	355	600
Estimate liquid cooling rate (Ks^{-1})	9200	1600	750	38200	13900	5300	2080

2.2. DSC experiments

DSC tests were carried out on IA powders of different size ranges (including the sizes corresponding to the powders analyzed by ND given in table 1) and gas atomized powders in order to measure the amorphous fractions in each powder based on the enthalpy of crystallization. The DSC experiments were performed by heating 30mg of powders in each size range of interest with a temperature ramp of $20Kmin^{-1}$ from room temperature to 1500K in a Setaram Labsys Evo 1600 Differential Scanning Calorimeter under a flow of high purity argon. Prior to the tests, the instrument was calibrated for temperature and heat measurement for the entire temperature range using standard samples of Sn, Zn, Al, Ag, Au and Ni. The amorphous fraction in each IA powder was measured by relating their enthalpy of crystallization to the enthalpy of crystallization of the GA (reference) powders that are close to fully amorphous according to the diffraction data. A detail description of the DSC experiments and details on the estimation of amorphous fraction from the enthalpy of crystallization is given in [4].

2.3. ND experiments

ND was performed on IA as well as on GA (reference) powders to measure the average weight fraction of microstructural phases. About 2-3 grams of powders from size ranges corresponding to different cooling rates were analyzed. The experiments were conducted using the C2 neutron powder diffractometer located at the Canadian Neutron Beam Centre (CNBC) in Chalk River, ON, Canada. The C2 neutron powder diffractometer is equipped with an 800-wire BF3 position sensitive detector that floats on an epoxy resin floor. A neutron wavelength of 1.33 Å taken from a Si531 monochromator was used for measurements. The powders were placed inside a vanadium can of 5mm internal diameter, and 1 cm^3 volume. Beam-defining slits were used to illuminate only the sample volume.

3. Results

3.1. Amorphous fraction obtained by DSC Fig.2 shows a plot of amorphous fraction variation with powder size and cooling rate for the as-atomized powders both in H and in N atmospheres. In agreement with results presented in Fig.1, and as expected, vitrification is promoted by high cooling rate [1]. Fig.2a & 2b show that the amorphous fraction increases as the average powder size decreases or the average cooling rate increases. For two powders of the same size, H-atmosphere atomization is found to yield a higher fraction of amorphous phase.

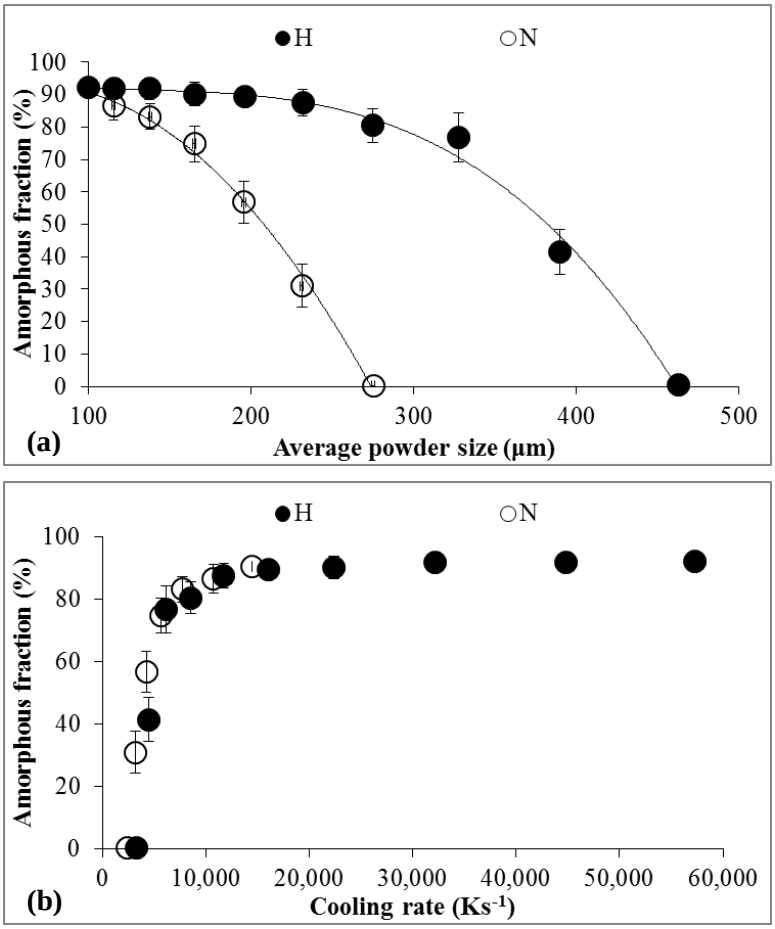

Fig.2: *DSC measured amorphous fraction as a function of (a) average powder size, (b) liquid cooling rate. H and N mean atomized under helium and nitrogen respectively*

Indeed, to generate the same amorphous fraction by IA, the ratio of powder size atomized under H and under N is about ½. Furthermore, in Fig.2a, the slope of the curve "Amorphous fraction *Vs* Average powder size" is found to be steeper for N as compared to H, indicating that the crystallization process for powders atomized in H is slower than the ones atomized in nitrogen. In addition, both curves show a maximum of ~90% amorphous fraction obtained at a cooling

rate of about 15,000Ks^{-1} which corresponds to 100μm and 200μm IA powders in N and H, respectively.

3.2. Amorphous fraction obtained by Neutron Diffraction (ND)

Fig.3 shows ND patterns (Intensity Vs Q) of the investigated powders. Q is defined as $Q = 4*\pi / \lambda*\sin(\theta)$ where λ is the neutron wavelength and 2θ is the scattering angle. Rietveld refinement method [8] was performed using the software GSAS (General Structure Analysis System) in order to identify and quantify the different crystalline phases present in the powders.

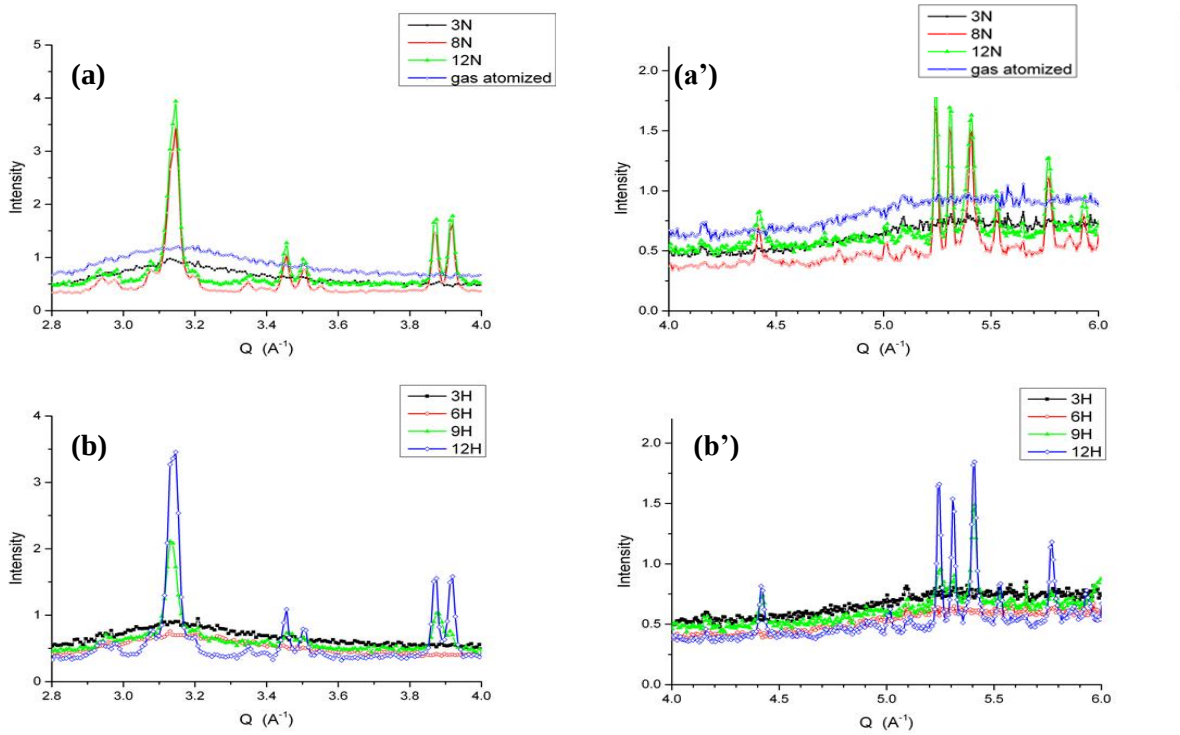

Fig.3: *Diffraction patterns obtained from the neutron diffraction measurements conducted using the C2 neutron powder diffractometer at Canadian Neutron Beam Centre (NRC-CNBC) in Chalk River, ON. (a-a') powders atomized in N, (b-b') Powders atomized in H. Patterns of a close to amorphous reference powder (gas atomized) are plotted for comparison.*

The positions of the observed oscillations in the ND patterns for the reference (gas atomized sample) are compatible with the amorphous phases found in the $Fe_{43.2}Co_{28.8}B_{19.2}Si_{4.8}Nb_4$ BMG processed by the wedge mold casting technique (cooling rates in the range 10^1–10^2 Ks^{-1}) and the $Fe_{65}Co_{21}B_{15}$ samples rapidly solidified by melt-spun ribbon technique (cooling rates in the range 10^4–10^7 Ks^{-1}), results presented respectively in [9] and [10]. The same crystalline phases (within statistical errors) are found in samples atomized both in H and N (cooling rates in the range 10^2–10^4 Ks^{-1}). In both references [9] and [10] as well as in a melt-spun $Fe_{67}Co_{18}B_{14}Si_1$

ribbon [11] α-(FeCo) could be identified while this phase seems to be absent in the investigated IA powders produced both in H and in N atmospheres (Fig.4).

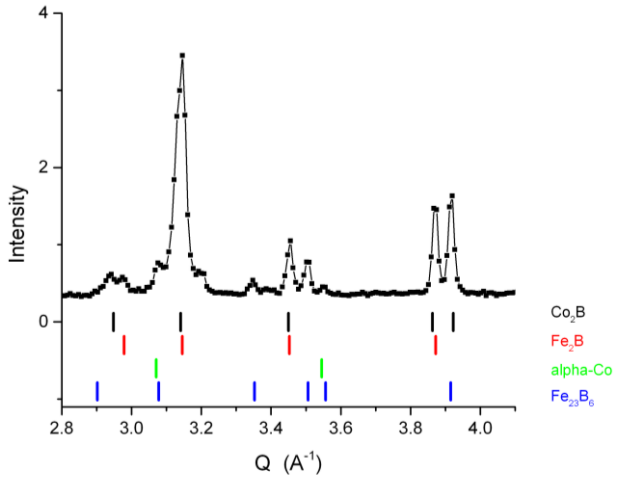

Fig.4: *Results of Rietveld refinement analysis of the diffraction patterns for powders with average droplet size of 600μm atomized under H. Phases corresponding to each peak have been identified by the software GSAS (General Structure Analysis System)*

The vertical bars in Fig.4 shows the diffraction peak positions of the nucleated phases in both IA powders (Co_2B, Fe_2B, and $Fe_{23}B_6$) that were also identified in [12]. Compared with tabulated lattice dimensions, the Co_2B phase is found to be slightly distorted (the a-axis 0.04Å longer and the c-axis 0.03Å shorter than the tabulated values) while the Fe_2B lattice cell is found to be 0.7% larger. The lattice constant calculated for the $Fe_{23}B_6$ phase is found to be 10.60 which is comparable with 10.73 given in [13]. Thus the compositions of the phases probably are not the nominal ones. Phase growth is somewhat different in the samples atomized in H and in N. It can be concluded that the ratio of the amounts of Co_2B and Fe_2B phases varies during their growth but the data are not accurate enough to quantitatively make any statistical conclusion based on the measured diffraction patterns. It is however clear that the lattice dimensions change during growth.

3.3. Amorphous fractions comparison: ND Vs DSC

Fig.5 shows a comparison between the amounts of crystalline fractions in the powders atomized in both N and H as obtained by Rietveld refinement of the ND patterns and from the DSC measurements.

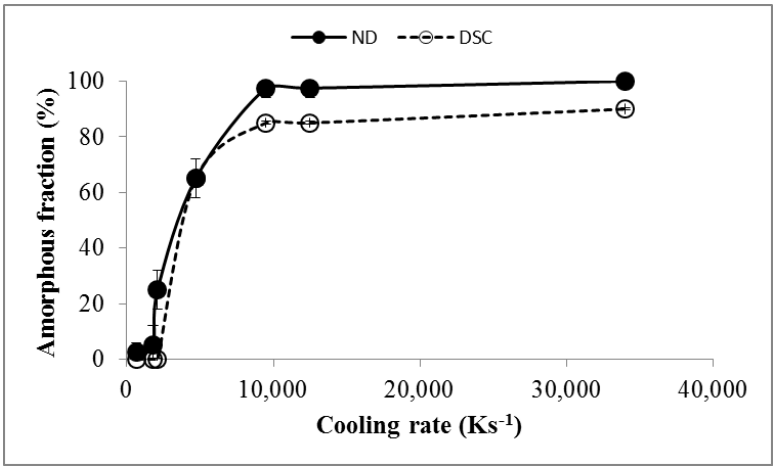

Fig.5: *Amorphous fraction variation with cooling rate estimated from the neutron diffraction (ND) and from the Differential Scanning Calorimetry (DSC)measurements*

It can be seen that at low cooling rate (<10,000Ks^{-1}) both ND and DSC predict the same amorphous fraction. Above 10,000Ks^{-1} ND yields higher amorphous fractions than DSC. 100% amorphous fraction is obtained around 15,000Ks^{-1}. Indeed, at relatively low cooling rates/large powder size the undercooling is generally relatively lower which makes the incubation time for precipitation upon heating shorter and the enthalpy of crystallization more detectable. At higher cooling rates generally characterized by high undercooling and high amorphous fraction, the precipitation of crystalline phases upon heating is slower and not fully detected by DSC, resulting in lower estimated fractions of amorphous phase. However, ND which relates directly to the atomic structure of matter is more appropriate in yielding an accurate estimation of amorphous phases in a material. This observation also suggests that the crystallization process is slower for powders atomized in H (Higher cooling rate and therefore slower incubation time for crystallization upon heating) as compared to the ones atomized in N. Another reason that might explain the difference in amorphous fraction given by DSC and ND is likely that the investigated mass by ND is 100 times larger than that analyzed by DSC so that a more accurate result is like to be obtained by ND which is considerably higher than that obtained in the constrained solidification condition reported in the literature [9]–[11].

3.4. Mechanical properties: Vickers micro-hardness

Vickers micro-hardness measurements were carried-out on as-atomized powders of different sizes/ cooling rates. Two indentations, at a distance from each other equivalent to 3 times the diameter of one indentation, were randomly applied on each ground and polished powder surface using a 50gf test force and held for 5 sec. Five powders were tested in each investigated size range.

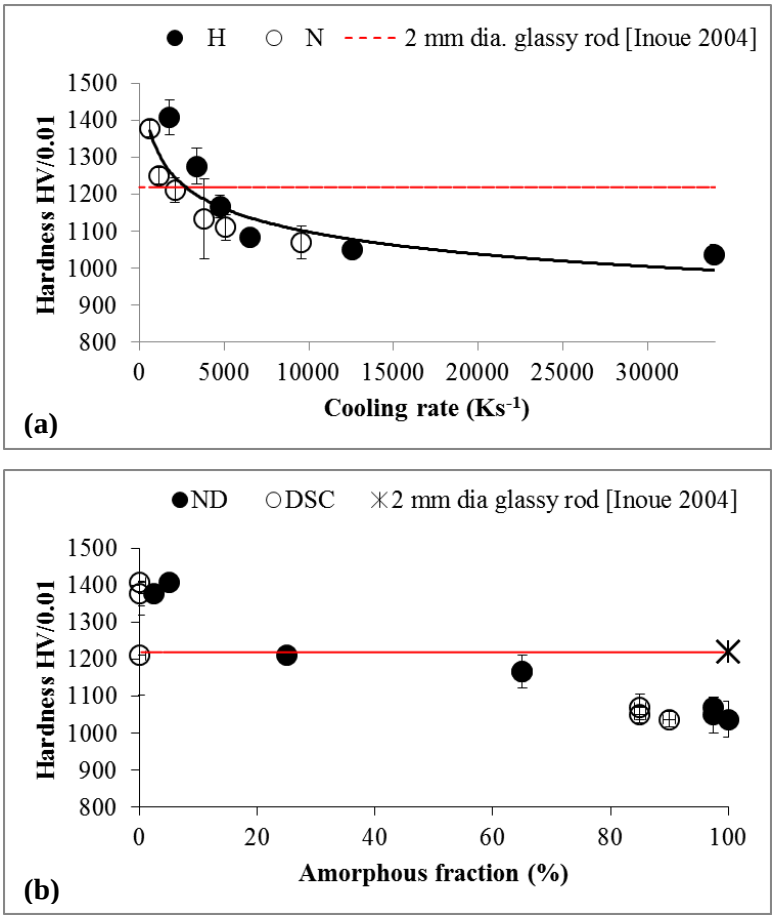

Fig.6: *Variation of Vickers micro-hardness of* $\{(Fe_{60}Co_{40})_{75}B_{20}Si_5\}_{96}Nb_4$ *powders obtained by IA in H and in N (a) with estimate liquid cooling rate by a thermal model* [7] *(b) with estimated amorphous fraction by DSC and ND. The results are compared with the hardness of a fully amorphous rod of the same compositions* [3](*indicated by the horizontal line).*

Fig.6 shows Microhardness variation with cooling rate and amorphous fraction. It can be seen that there is a general decrease of hardness with cooling rate and amorphous fraction from a maximum value of about 1400 Hv corresponding to a fully crystalline powder to a minimum value of about 1000 Hv in a fully amorphous powder. Fig.6a shows hardness variation with cooling rate (or average powder size). It can be seen that hardness decreases (or increases) with cooling rate (or average powder size). This observation suggests that the amorphous phases are softer than the crystalline structures, in agreement with measurements reported in [4]. For samples of average cooling rate below 2100 Ks^{-1} (average powder size of 300µm in nitrogen) or amorphous fraction below 25% (Fig.6b), hardness is higher than the reported 1225 Hv for a 2 mm in diameter glassy rod with the same composition obtained by the copper mold casting method [3]).

4. Conclusions

Amorphous phase formation under unconstrained solidification conditions was analyzed through $\{(Fe_{60}Co_{40})_{75}B_{20}Si_5\}_{96}Nb_4$ powders generated by Impulse Atomization in Nitrogen and Helium atmospheres. Cooling rates corresponding to each IA powder were estimated by a thermal model for Impulse Atomization. Calorimetry and Neutron diffraction were used to estimate the amorphous fraction for selected powders of different size ranges. The fractions are found to vary with powder size and cooling rate. As expected, the higher cooling rate generated in helium atmosphere is found to yield higher amorphous fraction. The crystalline phases identified by Rietveld refinement of Neutron Diffraction data are found to be consistent with the ones reported in literature except for the α-(FeCo) which has not been identified in the present investigation likely due to the high undercooling and high cooling rate induced solidification. The critical cooling rate for a fully amorphous powder generated under unconstrained solidification conditions in nitrogen and helium by IA corresponds to a powder size of 100 μm and 200 μm, respectively.

Acknowledgements

The authors are grateful to the Natural Sciences and Engineering Research Council of Canada (NSERC), for financial support. Access to neutron scattering beam time at the Canadian neutron Beam Centre in Chalk River, ON, Canada is also acknowledged.

References

[1] W. KLEMENT, R. H. WILLENS, and P. DUWEZ, "Non-crystalline Structure in Solidified Gold–Silicon Alloys," *Nature*, vol. 187, no. 4740. pp. 869–870, 1960.

[2] H. Henein, "Single fluid atomization through the application of impulses to a melt," *Mater. Sci. Eng. A*, vol. 326, no. 1, pp. 92–100, Mar. 2002.

[3] A. Inoue, B. L. Shen, and C. T. Chang, "Super-high strength of over 4000 MPa for Fe-based bulk glassy alloys in [(Fe1−xCox)0.75B0.2Si0.05]96Nb4 system," *Acta Mater.*, vol. 52, no. 14, pp. 4093–4099, Aug. 2004.

[4] V. Ciftci, N. Ellendt, N.Von Bargen, R.Henein, H. Mädler, L.Uhlenwinkel, "Atomization and characterization of a glass forming alloy {(Fe 0.6Co0.4)0.75B0.2Si 0.05}96Nb4," *J. Non. Cryst. Solids*, vol. 394–395, pp. 36–42, 2014.

[5] S. Lagutkin, L. Achelis, S. Sheikhaliev, V. Uhlenwinkel, and V. Srivastava, "Atomization process for metal powder," *Mater. Sci. Eng. A*, vol. 383, no. 1 SPEC. ISS., pp. 1–6, 2004.

[6] J. B. Wiskel, K. Navel, H. Henein, and E. Maire, "Solidification study of aluminum alloys using Impulse Atomization: Part II. Effect of cooling rate on microstructure," in *Canadian Metallurgical Quarterly*, 2002, vol. 41, no. 2, pp. 193–204.

[7] A. Prasad, S. Mosbah, H. Henein, and C.-A. Gandin, "A Solidification Model for Atomization," *ISIJ International*, vol. 49, no. 7. pp. 992–999, 2009.

[8] D. Balzar and N. C. Popa, "Analyzing microstructure by rietveld refinement *," *Rigaku J.*, vol. 22, no. 1, pp. 16–25, 2005.

[9] C. T. Rios, C. R. M. Afonso, C. Bolfarini, W. J. Botta F., and C. S. Kiminami, "Characterization of Glass Forming Alloy $Fe_{43.2}Co_{28.8}B_{19.2}Si_{4.8}Nb_4$ Processed by Spray Forming and Wedge Mold Casting Techniques," *Mater. Sci. Forum*, vol. 691, pp. 23–26, Jun. 2011.

[10] U. Dahlborg and M. Calvo-Dahlborg, "Influence of the production conditions on the structure and the microstructure of metallic glasses studied by neutron scattering," *Mater. Sci. Eng. A*, vol. 283, no. 1–2, pp. 153–163, 2000.

[11] E. Nunes, J. C. . Freitas, R. . Pereira, A. . Takeuchi, C. Larica, E. . Passamani, and A. A. . Fernandes, "Phase transformation in iron/cobalt-based amorphous alloys revealed by thermal and magnetic techniques," *J. Alloys Compd.*, vol. 369, no. 1–2, pp. 131–135, Apr. 2004.

[12] M. Stoica, R. Li, A. R. Yavari, G. Vaughan, J. Eckert, N. Van Steenberge, and D. R. Romera, "Thermal stability and magnetic properties of FeCoBSiNb bulk metallic glasses," *J. Alloys Compd.*, vol. 504, no. SUPPL. 1, pp. S123–S128, Aug. 2010.

[13] M. Imafuku, S. Sato, H. Koshiba, E. Matsubara, and A. Inoue, "Crystallization behavior of amorphous Fe 90-XNb 10B X (X = 10 and 30) alloys," *Mater. Trans. JIM*, vol. 41, no. 11, pp. 1526–1529, 2000.